

Experimental Studies and Thermodynamic Optimization of the Ni-Bi System

G.P. Vassilev, X.J. Liu, and K. Ishida

(Submitted April 14, 2004; in revised form December 2, 2004)

Experimental studies by electron microprobe analyses, optical microscopy, and differential scanning calorimetry were performed. New data about the liquidus in the central and the Bi-rich regions were obtained. A narrow homogeneity region (about 50-52 at.% Bi) was found for the compound NiBi while the second intermediate phase in this system (NiBi₃) was stoichiometric. Thermodynamic optimization of the Ni-Bi phase diagram was achieved by the CALPHAD method by combining phase diagram and thermodynamic data. Thus, NiBi was modeled with two sublattices, allowing mixing of Bi and Ni on one of them only. The intermetallic phase NiBi₃ was modeled as a stoichiometric compound. Redlich-Kister polynomials were used to describe the excess Gibbs energies of the solution phases (liquid, pure bismuth, and Ni-based solid solutions).

1. Introduction

The binary Ni-Bi alloys are technologically important for control of coating thickness during galvanizing processes of silicon-containing steels [2002Fra]. Some time ago, the Ni-Bi system was studied in relation to the superconducting properties of the compound NiBi₃ [1963Zhu, 1966Mat]. Knowledge of the phase equilibria in this system is important in view of eventual application of lead-free Bi-containing solders on nickel substrates.

Two stable compounds exist in the Ni-Bi system: NiBi₃ and NiBi. All authors agree that the first is stoichiometric while the second exhibits a small homogeneity region. In any case, the phase diagram compiled by Predel [1992Pre] differs from the one of Nash [1991Nas] and Masalski [1996Mas], concerning the NiBi-phase homogeneity range and the liquidus topology at more than about

50 at.% Bi. Consequently, the Ni-Bi phase diagram needs further investigation. Thus, the purpose of the present work was to study experimentally some contentious parts of the Ni-Bi system as well as to perform a thermodynamic optimization.

2. Phase Diagram and Thermochemical Data Review

Portevin [1908Por] and Voss [1908Vos] constructed the liquidus in the central and Ni-rich side of the system by thermal analysis method (studying the cooling curves). Both authors have accepted the Ni melting point as 1724 K (i.e., a 4 K difference from the contemporary value of 1728 K [1996Mas]). The Bi melting point has been acknowledged as 542 K, about 2° below the presently accepted value. Another possible source of error (change of the chemical composition of the specimens) is connected with the relatively high Bi vapor pressure (boiling point 1837 K) because the experiments have been performed in open crucibles. Thus, bearing in mind other uncertainties intrinsic to the temperature and thermal effects measurements, errors on the order of 10-20° could be attributed to the above cited

G.P. Vassilev, University of Sofia, Faculty of Chemistry, 1164 Sofia, Bulgaria; X.J. Liu and K. Ishida, Department of Materials Science, Graduate School of Engineering, Tohoku University, Aoba-yama 02, Sendai 980-8579, Japan. Contact e-mail: gpvassilev@excite.com.

Table 1 Composition intervals and crystal structures of the equilibrium Ni-Bi solid phases

Phase(a)	Approximate concluding interval, at.% Bi	Pearson symbol	Space group	Strukturbericht designation	Prototype	Reference
(Ni)	~0.05	<i>cF4</i>	<i>Fm</i> $\bar{3}m$	A1	Cu	[1996Mas]
NiBi	45-49(b,c)	<i>hP4</i>	<i>P6</i> ₃ / <i>mmc</i>	B8 ₁	NiAs	[1930Hag],[1963Zhu] [1988Fes],[2003Vil]
NiBi ₃	75	<i>oP16</i>	<i>Pnma</i>	<i>D</i> ¹⁶ _{2h}	CaLiSi ₂	[1953Zhd],[1969Kuz] [1987Fje],[2003Vil]
(Bi)	100	<i>hR2</i>	<i>R</i> $\bar{3}m$	A7	α As	[1996Mas]

(a) Metastable phases on the base of (Bi) and (Ni) have been reported [1975Kum]. (b) Approx. 50-51 at.% Bi [1988Fes]. (c) Approx. 50 ± 1.3 at.% Bi additionally reported [2001Obe].

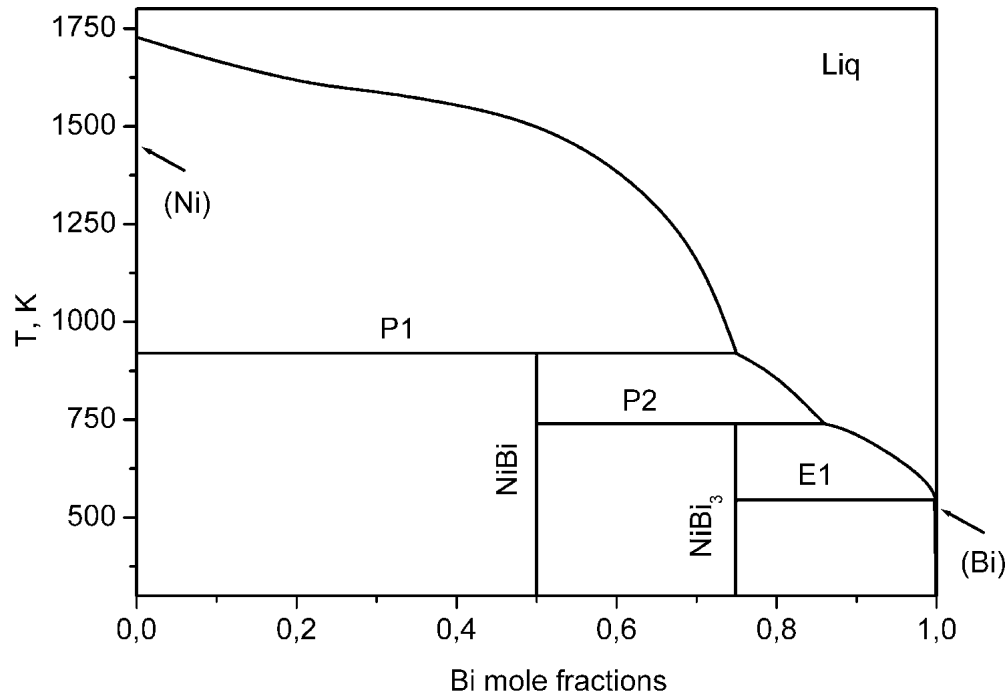


Fig. 1 The compiled Ni-Bi phase diagram [1992Pre]. The temperatures of the invariants are as follows: 918 ± 2 K for P1, 738 ± 2 K for P2, and 544 ± 1 K for E1.

results. The studies of Hägg and Funke [1930Hag] on the structure and stoichiometry of the nickel-bismuth solid compounds (Table 1) were also significant for the knowledge of the phase diagram.

More recently, Feschotte and Rosset [1988Fes] obtained by differential thermal analyses (again in open crucibles), data about the liquidus in the range from around 50-75 at.% Bi. Heating curves (100° h^{-1}) have been used. They also found (by means of x-ray diffraction and by microprobe analyses) that the NiBi-phase exhibits a homogeneity range. The latter is 51 ± 0.3 at.% Bi, while other sources [1991Nas, 1996Mas] attribute to this compound around 46 at.% Bi.

In Fig. 1, the Ni-Bi phase diagram is plotted as suggested by Feschotte and Rosset [1988Fes] and accepted by Predel [1992Pre]. Additional experimental information about the invariants in the Ni-Bi phase diagram is presented in Table 2. The Ni solubility in the rhombohedral Bi lattice is undoubtedly very small, while Bi solubility in the face-centered-cubic (fcc) Ni is around 1×10^{-2} to 1×10^{-4} mol%, according to various sources (Table 2). Enhanced Bi content (up to 0.199 mol fractions of Bi) was observed in electro-deposited fcc Ni-Bi alloys [1975Kum] but those authors admit that such a large solubility corresponds to a nonequilibrium state.

The phase relations in the BiNi-Pd system were investigated by Oberndorff et al. [2001Obe] using diffusion couples and equilibrated alloys. An isothermal section at 235° C has been constructed. In the latter work, the NiBi-phase is represented as having homogeneity ranges in the interval 50 ± 1.3 at.% Bi (see Fig. 6 of that reference). This is like the homogeneity range found by Feschotte and Rosset [1988Fes].

Table 2 Experimental and calculated data for the invariant points in the Ni-Bi phase diagram

Reaction(a)	T(b), K	X^{LS} (c)	X^{M} (d)	X^{RS} (e)	Reference
Peritectic, P1	913	-0.005	-0.5	-0.693	[1908Vos]
	927	?	-0.5	-0.802	[1908Por]
NiBi(f) \rightarrow (Ni)(g) + L	913	-0.005	-0.450	-0.680	[1930Hag]
	927	[1969Kuz]
(f)	919 ± 2	0.0007	0.51	-0.75-0.76	[1988Fes]
	926	This work
	918.9	0.0049	0.512	0.814	A.V.(h)
Peritectic, P2	748	-0.5	-0.75	-0.907	[1908Vos]
	735	-0.5	0.75	-0.901	[1908Por]
NiBi ₃ \rightarrow NiBi + L	753	-0.463	0.75	-0.812	[1930Hag]
	743	[1969Kuz]
	738 ± 2	-0.51	0.75	-0.86	[1988Fes]
Eutectic, E1	737.9	0.514	0.75	0.913	A.V.
	543	[1908Vos]
	542	[1908Por]
NiBi ₃ \rightarrow (Bi) \rightarrow L	543	[1969Kuz]
	543.35	0.75	0.9947	1	[1979Sha]
	544 ± 1	[1988Fes]
	543.0	0.75	0.9934	1	A.V.

(a) All reactions are written as in heating; (b) temperature; (c) Bi mole fraction; Ni-rich side point; (d) Bi mole fraction, middle point; (e) Bi mole fraction, Bi-rich side point; (f) previously suggested homogeneity ranges are $X_{\text{Bi}} = 0.463-0.443$ [1930Hag], $0.488-0.452$ [1996Mas], $0.509-0.512$ [1988Fes] by EMPA, and $0.50-0.51$ by chemical analyses; this work (by EMPA), $0.505-0.515$; (g) The bismuth solubility in (Ni)-phase according to various authors is $X_{\text{Bi}} = 0.005$ [1908Vos], 0.015 [1958Kor], 0.0007 [1988Fes], this work (by EMPA): 1×10^{-2} to 1×10^{-3} (this work) (h) assessed in this work.

Table 3 Overall chemical composition and heat treatment details for the studied alloys

No	$X_{Bi}(a)$	$T(b), K$	Time(c), days	Notes(d)
1	0.750	781	7	Ni(sh)(e)
		887	5	$m = 9.5$ g
		674	6	...
2	0.525	781	7	Ni(sh)
		887	18	$m = 7.5$ g
3	0.472	887	20	Ni(p)(f)
		617	3	$m = 6.0$ g
4	0.505	887	21	Ni(p)
				$m = 5.5$ g
5	0.219	1371	5	Ni(b)(g)
				$m = 1.7$ g
6	0.598	887	9	Ni(b)
		1273	1	$m = 6.5$ g
		887	6	...
7	0.205	1273	1	Ni(b)
		962	7	$m = 3.5$ g
8	0.701	887	9	Ni(b)
		1080	1	$m = 3.5$ g
		617	7	...
9	0.221	1283	8	Ni(b)
				$m = 2.0$ g
10	0.400	1473	2	Ni(sh)
		887	15	$m = 1.7$ g
11	0.398	1473	2	Ni(sh)
		781	15	$m = 1.7$ g
12	0.070	1473	11	Ni(sh)
				$m = 1.3$ g
13	0.102	1593	3	Ni(sh)
				$m = 1.3$ g
14	0.225	1473	3	Ni(sh)
		1578	2	$m = 1.97$ g
15	0.274	1473	3	Ni(sh)
		1373	2	$m = 1.97$ g
16	0.220	1523	5	Ni(sh)
				$m = 1.97$ g

(a) Bi mole fraction of the specimen; (b) annealing temperature; (c) duration of annealing; (d) m , the appropriate mass of the specimen; (e) Ni(sh), Ni sheets, 0.2 mm thick; (f) Ni(p), Ni powder; (g) Ni(b), bulk Ni.

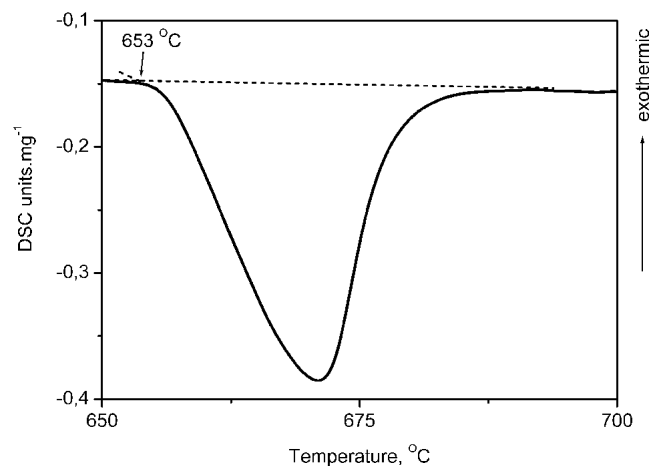


Fig. 2 DSC curve (heating rate $10^\circ \text{ min}^{-1}$) of specimen 3. The peak at around 653° C (926 K) is due to the peritectic melting of the compound NiBi.

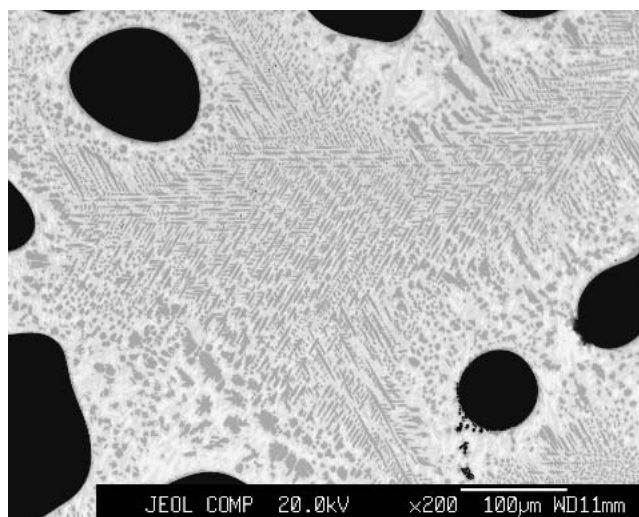


Fig. 3 Micrograph (in characteristic X-rays) of specimen 16. The alloy is two-phase $\{(Ni) + \text{liquid}\}$ at the annealing temperature (1523 K). The black areas are (Ni) particles, while the white regions correspond to almost pure Bi. A large amount of Ni-rich dendrites can be seen between them.

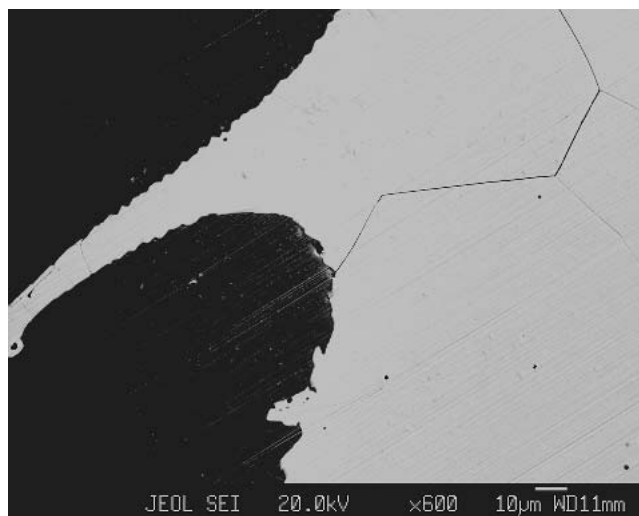


Fig. 4 Micrograph (in backscattered electrons) of specimen 10. The alloy is two-phase $\{(Ni) + NiBi\}$ at the annealing temperature (887 K). The dark areas correspond to the (Ni) phase; the light matrix (where grain boundaries can be distinguished) correspond to the compound NiBi.

Iwase and McLean [1983Iwa] measured the nickel thermodynamic activities in Bi-rich liquid solutions (in the range $970\text{--}1170 \text{ K}$) using an electro-motive force (EMF) technique. Nonetheless, experimental data for the Ni activities at 1073 K and an extrapolation to 1773 K have been published.

3. Experimental Studies

Sixteen Ni-Bi alloys were synthesized using pure components (4N). Ni-sheets 0.2 mm thick, Ni-powder, and bulk Ni were used, while the bismuth was in the form of pellets.

Section I: Basic and Applied Research

Table 4 Summarized results from the experimental studies of the Ni-Bi system

No.	Phases(a)	N.M.(b)	Composition S.D.(c),(d)	T.A.(e), K	Note
1	NiBi ₃	11 (f.s.)(f)	0.744 ± 0.004	674	Point analyses are used; a few confined Bi-rich inclusions (liquid phase) are observed
		10 (s.s.)(g)	0.747 ± 0.002		
		All 21	0.746 ± 0.004		
	L	6	0.9964 ± 0.0012		
2	NiBi	7	0.507 ± 0.003	887	Point analyses are used Area analyses (100 × 100 m 10 ⁻⁶)
		L	8		
3	NiBi	11 (f.s.)	0.516 ± 0.003	617	One Ni-rich area found in each section. Thus, the specimen could be considered to be in equilibrium with (Ni).
		10 (s.s.)	0.503 ± 0.004		
		All 21	0.511 ± 0.007		
4	NiBi	10	0.509 ± 0.005	887	Point analyses are used; no inclusions of (Ni) or Ni-rich regions found.
5	L (Ni)	8	0.65 ± 0.01	1440	Area analyses (300 × 300 m 10 ⁻⁶) of the liquid phase
		2	~1 × 10 ⁻²		
6	NiBi	9	0.507 ± 0.002	887	Area analyses (70 × 70 m 10 ⁻⁶) of the liquid phase
		L	9		
7	L (Ni)	9	0.75 ± 0.01	962	Area analyses of the liquid phase (300 × 300 m 10 ⁻⁶)
		2	~1 × 10 ⁻²		
8	NiBi NiBi ₃	7	0.516 ± 0.007	617	The bright phase (NiBi ₃) is prevailing, in agreement with the lever law.
		10	0.748 ± 0.005		
9	L (Ni)	9	0.67 ± 0.02	1283	Area analyses of the liquid phase (300 × 300 m 10 ⁻⁶)
		2	~1 × 10 ⁻²		
10	NiBi (Ni)	6	0.516 ± 0.005	887	...
		8	(5 ± 3) × 10 ⁻⁴		
11	NiBi (Ni)	10	0.513 ± 0.005	781	...
		10	~1 × 10 ⁻³		
12	L	11	0.66 ± 0.09	1473	Area analyses (50 × 50 m 10 ⁻⁶) of the liquid phase
13	L	5	0.58 ± 0.12	1593	Area analyses (10 × 10 m 10 ⁻⁶) of the liquid phase
14	L (Ni)	14	0.47 ± 0.06	1578	Area analyses (100 × 100 m 10 ⁻⁶) of the liquid phase
		10	~1 × 10 ⁻²		
15	L (Ni)	10	0.56 ± 0.03	1373	Area analyses (100 × 100 m 10 ⁻⁶) of the liquid phase
		10	~1 × 10 ⁻²		
16	L (Ni)	10	0.64 ± 0.03	1523	Area analyses (100 × 100 m 10 ⁻⁶) of the liquid phase
		6	~1 × 10 ⁻²		

(a) Phases identified by EMPA; (b) number of measurements; (c) chemical composition (Bi mole fractions) of the identified phases and the standard deviation; (d) standard deviation of the results (for scatter of multiple analyses); (e) temperature of annealing; (f) first section; (g) second section of a specimen (where more than one section is studied)

Precisely weighed (to the fourth sign after decimal point) initial mixtures were put in quartz tubes, rinsed three times under vacuum (0.4-2 Pa) with pure argon, and sealed. The details about the overall compositions of the specimens and the thermal treatment applied are exhibited in Table 3. After isothermal annealing, the specimens were quenched in ice water. The phase and chemical compositions of the equilibrated specimens were obtained by means of optical microscopy and electron microprobe analyses (EMPA), making use of the wave dispersive system method. The apparatus was calibrated using pure metal standards. Sequential (not simultaneous) determination of the elements was done, thus ensuring low background and detectability limits of order or 100 ppm [2001Kod].

Differential scanning calorimeter (DSC) analysis of specimen No. 3 (containing 47.2 at.% Bi) was performed using a NETZSCH DSC 404C instrument (Netzsch, Germany). As a result, the NiBi peritectic melting temperature (Fig. 2) was found to be ≈653 °C (926 K), in good agreement with literature data (Table 2).

According to the literature sources (Table 2) the peritectic temperatures vary from 913 to 927 K for P1 [NiBi ↔ (Ni)+L] and from 735 to 753 K for P2 (NiBi₃ ↔ NiBi + L). Nevertheless, the differences can be reasonably explained taking into account that the measurements are done by various methods (e.g., analyzing cooling curves [1908Vos, 1908Por], and heating curves [1988Fes]). Moreover, Kuz'min and Nikitina [1969Kuz] have associated the peritectic temperatures with the peak maximums, while other authors might have used the bases of the peaks, a technique preferred today. For the calculation of the adjustable coefficients, the peritectic temperatures found by Feschotte and Rosset [1988Fes] have been retained.

In Fig. 3 and 4 are shown micrographs of specimens 16 and 10, respectively. The first alloy (annealed at 1523 K) is situated in the two-phase field (Ni) + liquid, while the second (annealed 887 K) is in the two-phase region (Ni) + NiBi.

It was found that the chemical composition of the compound NiBi determined by EMPA is comprised in the in-

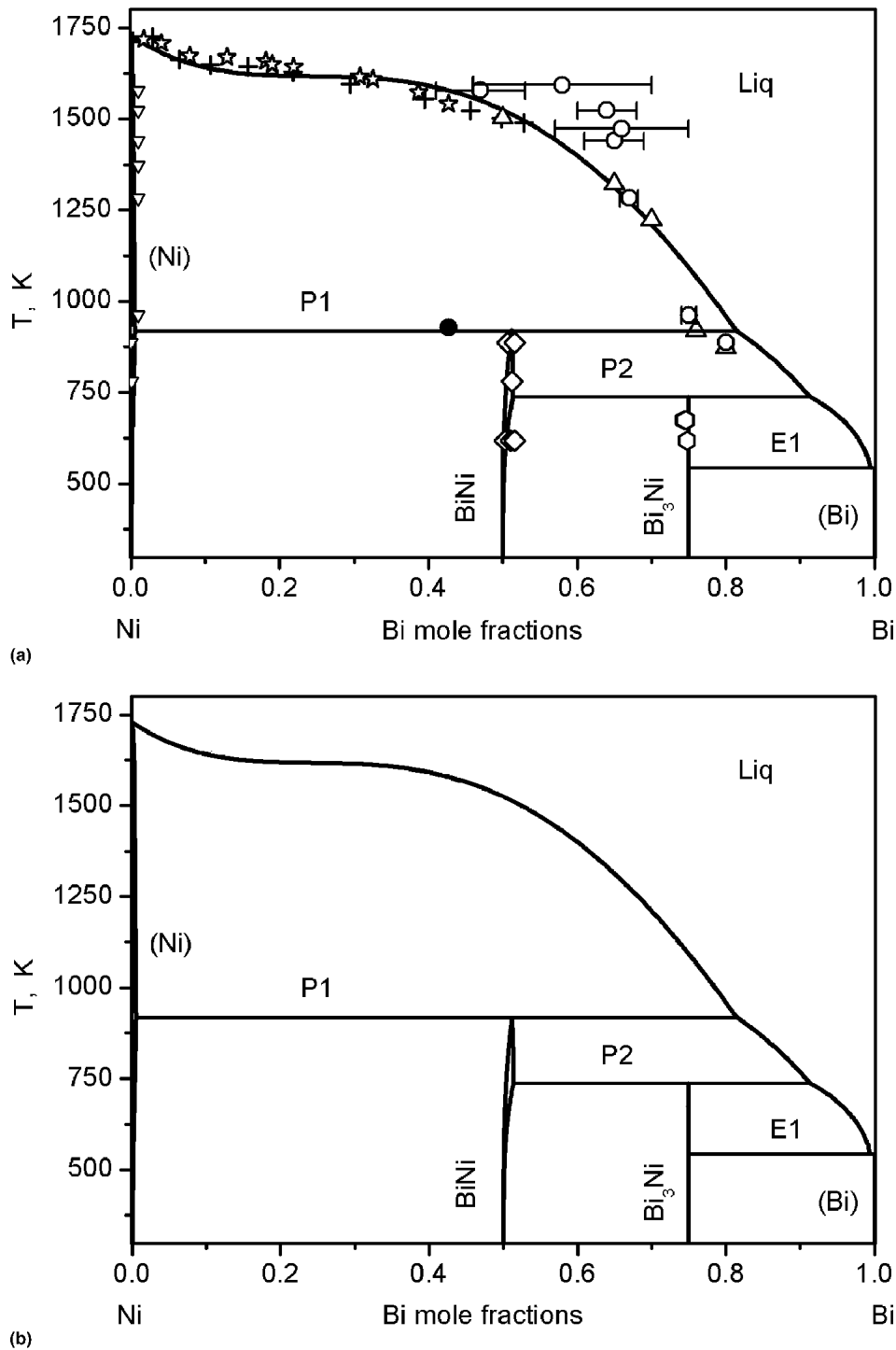


Fig. 5 (a) Phase diagram of the Ni-Bi system, calculated with the optimized coefficients. Literature experimental data points: (+) [1908Vos], (☆) [1908Por], (△) [1988Fes]. This work data: (o) liquidus; (∇) (Ni); (◇) NiBi; (○) NiBi₃; (●) peritectic melting of specimen 3. The standard deviations of the authors' liquidus points are represented as short lines. (b) Phase diagram of the Ni-Bi system, calculated in this work with the optimized coefficients. The following invariant temperatures are calculated: P1, 919 K; P2, 738 K; E1, 543 K.

terval 51 ± 1 at.% Bi (Table 4). This generally conforms with the data of Feschotte and Rosset [1988Fes] and of Oberndorff et al. [2001Obe] and confirms the existence of a small homogeneity region. We would like to emphasize that all evidences show that the compound is not exactly stoi-

chiometric, but is slightly displaced to the Bi-rich side at temperatures near the peritectic temperature.

Some information on the bismuth solubility in the solid nickel [(Ni)-phase] and the nickel solubility in liquid bismuth (liquidus line) were obtained as well (Table 4).

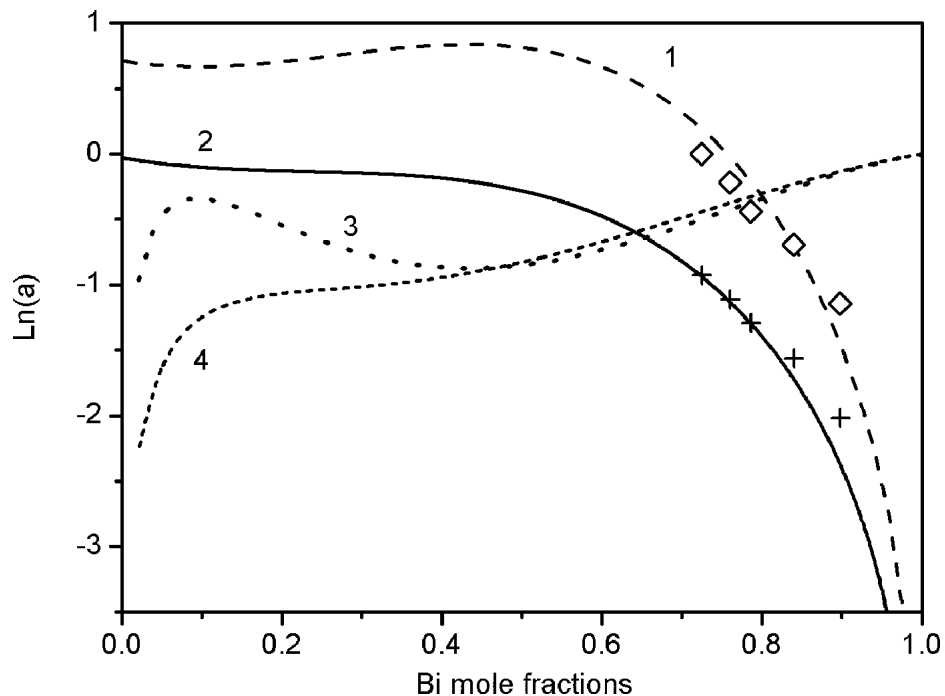


Fig. 6 Comparison of experimental and extrapolated data about the Ni-activities in the liquid solutions at 1073 K (\diamond) and 1773 K (+), respectively, [1983Iwa] with calculated in this work values: Line 1, Ni-activities at 1073; line 2, Ni-activities at 1773 K. The calculated Bi activities at the respective temperatures are represented by the lines 3 and 4. The Ni activities are referred to the pure fcc Ni (as are the original experimental data [1983Iwa]), while the Bi activities are referred to the pure liquid Bi. The natural logarithms of the activity values are plotted along the ordinate axis, and the Bi mole fractions are plotted along the abscissa.

4. Thermodynamic Modeling and Discussion

The thermodynamic parameters describing the Gibbs energies of the phases constituted by pure Ni and Bi, respectively, have been taken from the compilation of Dinsdale [1991Din]. The temperature dependencies of the molar Gibbs energies ($^{\circ}G_i$) for the pure elements are described in the form:

$$^{\circ}G_i(T) - ^{\circ}H_i^{\text{SER}} = A_i + B_iT + C_iT \ln T + D_iT^2 + E_i/T + F_iT^3 + I_iT^4 + J_iT^7 + K_iT^{-9} + \Delta G_{\text{mag}}(T) \quad (\text{Eq 1})$$

where $^{\circ}H_i^{\text{SER}}$ represents the enthalpy of the pure element (i), in its stable state, at the standard temperature 298.15 K and pressure 1 bar; T is the current temperature; and $\Delta G_{\text{mag}}(T)$ is the magnetic term.

The pertinent coefficients for the lattice stabilities of the pure rhombohedral Bi [phase (Bi)] are taken from an update of Dinsdale's compilation [1991Din] kindly supplied by Prof. H.L. Lukas (Table 5). No data about the lattice stabilities of the hypothetical rhombohedral Ni were found; thus a value of $+50 \text{ kJ mol}^{-1}$ was added to the lattice stabilities of the pure fcc Ni to make the rhombohedral Ni unstable enough.

The phases (Ni), liquid, and (Bi) were treated as disordered substitutional solutions. The Ni solubility in the rhombohedral (Bi)-phase is unknown but is supposed to be even less than the Bi solubility in the (Ni)-phase (the parentheses denote the pertinent phase, to distinguish it from the corresponding element). Thus, the calculations were

performed assuming zero nickel content in the (Bi)-phase (consequently, no interaction parameters are attributed to this phase).

The phase NiBi_3 was modeled as a stoichiometric compound with two sublattices $(\text{Ni})_{0.25}(\text{Bi})_{0.75}$. The compound energy formalism was applied for the description of the Gibbs energy of the nonstoichiometric NiBi phase. A variant with two sublattices $(\text{Bi})_{0.5}(\text{Ni}, \text{Bi})_{0.5}$ was used to reflect the fact that the bismuth is always predominant component.

During the first stage of the optimization work (performed with the PARROT module of THERMOCALC, KTH, Stockholm, Sweden), we estimated the adjustable parameters of the liquid solution and the (Ni)-phase, reproducing the high-temperature liquidus and solidus. In the second optimization step, the parameters of the intermetallic phases (NiBi and NiBi_3) were calculated. Lacking thermochemical data, only one temperature-independent parameter was assessed first (for each of the binary compounds). At the second stage of the optimization, linear temperature dependence (entropy term) was introduced to adjust the invariants' temperatures. Finally, all adjustable parameters (Table 5) were assessed simultaneously.

The Ni-Bi phase diagram constructed with the optimized coefficients is plotted in Fig. 5(a) (together with experimental information) and 5(b). As one can see, the scattering of the measured compositions of the liquid phase is large. The reason could be sought in the peculiarities of the Ni-Bi phase diagram (vertical phase boundary of the (Ni)) and the experimental method-equilibrium annealing and quenching.

Table 5 Thermodynamic database file (THERMOCALC compatible) for the pure elements and those calculated in this work thermodynamic parameters for the Ni-Bi system

Lattice Stabilities of the Pure Constituents	<i>BI3NI</i>
Functions	2 SUBLATTICES, SITES .75: .25
<i>GHSERBI</i>	CONSTITUENTS: BI, NI
298.14 < <i>T</i> < 544.54: -7817.776 + 128.418925* <i>T</i> -28.4096529* <i>T</i> *LN(<i>T</i>) + .012338888* <i>T</i> **2-8.381598E-06* <i>T</i> **3	G(BI3NI,BI:NI;0)-0.75*H298(RHOMBOHEDRAL_A7,BI;0) -0.25*H298(FCC_A1,NI;0) = 298.14 < <i>T</i> < 3000: -9562 + 4.721* <i>T</i> + 0.75 GBIHEX + .25*GNIHEX
544.54 < <i>T</i> < 800.00: +30,208.022-393.650351* <i>T</i> + 51.8556592* <i>T</i> *LN(<i>T</i>)	
-0.75311163* <i>T</i> **2 + 1.3499885E-05* <i>T</i> **3-3616168* <i>T</i> **(-1) + 1.661E+25* <i>T</i> **(-9)	<i>BINI</i>
800.00 < <i>T</i> < 1200.00: -11,045.664 + 182.548971* <i>T</i> -35.9824* <i>T</i> *LN(<i>T</i>) + .0074266* <i>T</i> **2-1.046E-06* <i>T</i> **3 + 1.661E + 25* <i>T</i> **(-9) Y	2 SUBLATTICES, SITES .5: .5
1200.00 < <i>T</i> < 3000: -7581.312 + 124.77144* <i>T</i> -27.196* <i>T</i> *LN(<i>T</i>) + 1.661E + 25* <i>T</i> **(-9)	CONSTITUENTS: BI, NI, BI
<i>GBILIQ</i>	G(BINI,BI:BI;0)-H298(RHOMBOHEDRAL_A7,BI;0) = 298.14 < <i>T</i> < 3000: +5000(a) + GBIHEX
298.14 < <i>T</i> < 544.54: +3428.29 + 107.782415* <i>T</i> -28.4096529* <i>T</i> *LN(<i>T</i>) + .012338888* <i>T</i> **2-8.381598E-06* <i>T</i> **3-5.955E-19* <i>T</i> **7	G(BINI,BI:NI;0)-0.5*H298(RHOMBOHEDRAL_A7,BI;0) -0.5*H298(FCC_A1,NI;0) = 298.14 < <i>T</i> < 3000: -7500 + 1.959* <i>T</i> + .5*GBIHEX + .5*GNIHEX
544.54 < <i>T</i> < 800.00: +41,544.282 - 414.460769* <i>T</i> + 51.8556592* <i>T</i> *LN(<i>T</i>) -0.75311163* <i>T</i> **2-3.616,168* <i>T</i> **(-1) + 1.3499885E-05* <i>T</i> **3	<i>BIRHOMB</i>
800.00 < <i>T</i> < 1200.00: +290.595 + 161.738553* <i>T</i> -35.9824* <i>T</i> *LN(<i>T</i>) + .0074266* <i>T</i> **2-1.046E-06* <i>T</i> **3	EXCESS MODEL IS REDLICH-KISTER_MUGGIANU
1200.00 < <i>T</i> < 3000: +3754.947 + 103.961022* <i>T</i> -27.196* <i>T</i> *LN(<i>T</i>)	2 SUBLATTICES, SITES 1: 1
<i>GBIHEX</i>	CONSTITUENTS: BI, NI: VA
298.14 < <i>T</i> < 3000: +9900-11.8* <i>T</i> + GHSERBI	G(BIRHOMB,BI:VA;0)-H298(RHOMBOHEDRAL_A7,BI;0) = 298.14 < <i>T</i> < 3000: +GHSERBI
<i>GHSERNI</i>	G(BIRHOMB,NI:VA;0)-H298(FCC_A1,NI;0) = 298.14 < <i>T</i> < 3000: +GNIRHOMB
298.14 < <i>T</i> < 1728.00: -5179.159 + 117.854* <i>T</i> -22.096* <i>T</i> *LN(<i>T</i>) -0.0048407* <i>T</i> **2	<i>FCC_A1</i>
1728.00 < <i>T</i> < 3000: -27,840.655 + 279.135* <i>T</i> -43.1* <i>T</i> *LN(<i>T</i>) + 1.12754E + 31* <i>T</i> **(-9)	EXCESS MODEL IS REDLICH-KISTER_MUGGIANU
<i>GNIBCC</i>	ADDITIONAL CONTRIBUTION FROM MAGNETIC ORDERING
298.14 < <i>T</i> < 3000: +8715.084 - 3.556* <i>T</i> + GHSERNI	Magnetic function below Curie Temperature
<i>GNILIQ</i>	+1 - .860338755*TAO**(-1) - .17449124*TAO**3 - .00775516624*TAO**9 - .0017449124*TAO**15
298.14 < <i>T</i> < 1728.00: +11,235.527 + 108.457* <i>T</i> -22.096* <i>T</i> *LN(<i>T</i>) -0.0048407* <i>T</i> **2-3.82318E-21* <i>T</i> **7	Magnetic function above Curie Temperature
1728.00 < <i>T</i> < 3000: -9549.775 + 268.598* <i>T</i> -43.1* <i>T</i> *LN(<i>T</i>)	-0.0426902268*TAO**(-5) - .0013552453*TAO**(-15) - 2.84601512E - 04*TAO**(-25)
<i>GNIRHOMB</i>	2 SUBLATTICES, SITES 1: 1
298.14 < <i>T</i> < 3000: +50,000(a) + GHSERNI	CONSTITUENTS: BI, NI: VA
<i>GNIHEX</i>	G(FCC_A1,BI:VA;0)-H298(RHOMBOHEDRAL_A7,BI;0) = 298.14 < <i>T</i> < 3000: +9900 - 12.5* <i>T</i> + GHSERBI
298.14 < <i>T</i> < 3000: +1046 + 1.2552* <i>T</i> + GHSERNI	G(FCC_A1,NI:VA;0)-H298(FCC_A1,NI;0) = 298.14 < <i>T</i> < 3000: +GHSERNI
Parameters assessed in this work:	TC(FCC_A1,NI:VA;0) = 298.14 < <i>T</i> < 3000: 633
Phase Liquid	BMAGN(FCC_A1,NI:VA;0) = 298.14 < <i>T</i> < 3000: .52
EXCESS MODEL IS REDLICH-KISTER_MUGGIANU	L(FCC_A1,BI,NI:VA;0) = 298.14 < <i>T</i> < 3000: +35* <i>T</i>
CONSTITUENTS: BI, NI	
G(LIQUID,BI;0)-H298(RHOMBOHEDRAL_A7,BI;0) = 298.14 < <i>T</i> < 3000: +GBILIQ	
G(LIQUID,NI;0)-H298(FCC_A1,NI;0) = 298.14 < <i>T</i> < 3000: +GNILIQ	
L(LIQUID,BI,NI;0) = 298.14 < <i>T</i> < 3000: +15,000 - 3.316* <i>T</i>	
L(LIQUID,BI,NI;1) = 298.14 < <i>T</i> < 3000: -17,000	
(a) - estimated values.	

It seems that the cooling was not fast enough to fix the high-temperature state, although the ampoules were submerged and broken in ice water. Thus, during cooling, the

quantity of (Ni) phase does not change, but Ni-rich dendrites appear as a result enriching the present liquid phase in bismuth.

Section I: Basic and Applied Research

In Fig. 6, the nickel activities in the liquid solutions at 1073 and 1773 K, calculated in this work, are juxtaposed with experimental data of Iwase and McLean [1983Iwa]. As one can see, both sources are in good agreement.

There is a trend of repulsion between Ni and Bi; thus the existence of an immiscibility region in the liquid phase was anticipated. Nevertheless, no experimental evidence of this was found.

5. Conclusions

Experimental investigation and thermodynamic optimization of the Ni-Bi system were performed. It was found that the homogeneity region of the intermediate phase NiBi is around 51 ± 1 at.% Bi while the compound NiBi₃ is stoichiometric. These data as well as the authors' data about the liquidus line are in general agreement with the results of Feschotte and Rosset [1988Fes]. Successful optimisation of the Ni-Bi system was achieved, although there is a lack of thermochemical data.

Acknowledgment

The authors gratefully acknowledge a fellowship provided to G.P.V. by the Japanese Society for the Promotion of Science.

References

- 1908Por:** M.A. Portevin, The Alloys of Nickel and Bismuth, *Rev. Metall.*, Vol 5, 1908, p 110-20 (in French)
- 1908Vos:** G. Voss, The Nickel-Bismuth System, *Z. Anorg. Chem.*, Vol 57, 1908, p 52-58 (in German)
- 1930Hag:** G. Hägg and G. Funke, X-ray Analysis of the System Ni-Bi, *Z. Phys. Chem. B*, Vol 6, 1930, p 272-283 (in German)
- 1953Zhd:** G.S. Zhdanov, V.P. Glagoleva, N.N. Zhuravlev, and Yu. N. Venetsev, Structure of Superconductors. I. Investigation of System Bi-Ni. Production and Investigation of Monocrystals Bi₃Ni, *Zh. Eksp. Teor. Fiz.*, Vol 25, 1953, p 115-122 (in Russian)
- 1958Kor:** I.I. Kornilov, *Nickel and Its Alloys*, Academy of Sciences of USSR, Ed. House of the Academy of Sciences of USSR, Moscow, USSR, 1958, p 11 (in Russian)
- 1963Zhu:** N. Zhuravlev, G. Zhdanov, and E. Smirnova, Study of Ternary Solid Solutions on the Basis of Superconducting Compounds, *Russ. J. Phys. Metall.*, Vol 13, 1962, p 62-70 (in Russian)
- 1966Mat:** B. Matthias, A. Jayaraman, T. Geballe, K. Andreas, and E. Gorenzvit, Many More Superconducting Bismuth Phases, *Phys. Rev. Lett.*, Vol 17 (No. 12), 1966, p 640-643
- 1969Kuz:** R.N. Kuz'min and S.V. Nikitina, Investigation of the Quasi-binary NiBi₃-RhBi₃ Section of Ni-Bi-Rh System, *Izv. Akad. Nauk SSSR, Metall.*, Vol 4, 1969, p 215-217 (in Russian); *Trans.: Russ. Metall.*, Vol 4, 1969 p 139-141
- 1975Kum:** P. Kumar and Y.N. Sadana, Electrodepositing of Alloys IV. Electrodepositing and X-ray Structure of Bismuth-Nickel Alloys from Aqueous Solutions, *J. Less-Comm. Metals*, Vol 43, 1975, p 259-265
- 1979Sha:** B.M. Shavinski, P.I. Artyukhin, and Yu. L. Mityakin, Directional Crystallization of Bismuth. III. Determination of the Eutectic Concentration of Some Metals in the Pure Bismuth Region, *Izv. Sibir. Otd. Nauk*, Vol 5, 1979, p 70-74 (in Russian)
- 1983Iwa:** M. Iwase and A. McLean, Activities in Nickel-Bismuth Alloys, *Metall. Trans. B*, Vol 14B, 1983, p 765-767
- 1987Fje:** H. Fjellvag and S. Furuseth, Structural Properties of Ni_{1-x}Rh_xBi₃, *J. Less-Com. Met.*, Vol 128, 1987, p 177-183
- 1988Fes:** P. Feschotte and J.M. Rosset, Phase Equilibria in the Binary Nickel-Bismuth System, *J. Less-Com. Met.*, Vol 143, 1988, p 31-37 (in French)
- 1991Din:** A.T. Dinsdale, SGTE Data for Pure Elements, *CAL-PHAD*, Vol 15, 1991, p 317-425
- 1991Nas:** *Phase Diagrams of Binary Nickel Alloys*, P. Nash and A. Nash, Ed., ASM, 1991, p 310
- 1992Pre:** B. Predel, in Landolt-Bornstein, *Numerical Data and Functional Relationships in Science and Technology*, New Series, O. Madelung, Ed., Group IV: Macroscopic and Technical Properties of Matter, Vol 5, *Phase Equilibria, Crystallographic and Thermodynamic Data of Binary Alloys*, Subvolume b, B-Ba...C-Zr, Springer-Verlag, Berlin, 1992, p 211-212
- 1996Mas:** T. Massalski, *Binary Alloy Phase Diagrams*, CD-ROM, ASM International, 1996
- 2001Kod:** A. Kodentsov, G. Bastin, F. Loo, The Diffusion Couple Technique in Phase Diagram Determination, *JALCOM*, Vol 320, 2001, p 207-217
- 2001Obe:** P.J.T.L. Oberndorff, M.G.A. van Vinken, A.A. Kodentsov, and F.J.J. van Loo, Phase Relations in the Bi-Ni-Pd System at 235 °C, *J. Phase Equil.*, Vol 22 (No. 3), 2001, p 265-268
- 2002Fra:** R. Fratesi, N. Ruffini, M. Malavolta, and T. Bellezze, Contemporary Use of Ni and Bi in Hot-Dip Galvanizing, *Surf. Coating Technol.*, Vol 157, 2002, p 34-39
- 2003Vil:** *Pauling File Binaries Edition. Inorganic Materials Database and Design System*, CD-ROM, P. Villars, Ed., Japan Science and Technology Corporation (JST) and Material Phases Data System (MPDS), ISBN 3-000-0090436, Germany, 2003.